Membrane-Bound and Exosomal Metastasis-Associated C4.4A Promotes Migration by Associating with the α6β4 Integrin and MT1-MMP[1,2]

Honoré Ngora[*,3], Uwe M. Galli[*,3,4], Kaoru Miyazaki[†] and Margot Zöller[*,‡]

[*]Department of Tumor Cell Biology, University of Heidelberg, Heidelberg, Germany; [†]Yokohama City University, Yokohama, Japan; [‡]German Cancer Research Center, Heidelberg, Germany

Abstract
Metastasis-associated C4.4A, which becomes upregulated during wound healing and, in some tumors, during tumor progression, is known to be frequently associated with hypoxia. With the function of C4.4A still unknown, we explored the impact of hypoxia on C4.4A expression and functional activity. Metastatic rat and human tumor lines upregulate C4.4A expression when cultured in the presence of $CoCl_2$. Although hypoxia-inducible factor 1α (HIF-1α) becomes upregulated concomitantly, HIF-1α did not induce *C4.4A* transcription. Instead, hypoxia-induced C4.4A up-regulation promoted *in vivo* and *in vitro* wound healing, where increased migration on the C4.4A ligands laminin-111 and -332 was observed after a transient period of pronounced binding. Increased migration was accompanied by C4.4A associating with α6β4, MT1-MMP1, and TACE and by laminin fragmentation. Hypoxia also promoted the release of C4.4A in exosomes and TACE-mediated C4.4A shedding. The association of C4.4A with α6β4 and MT1-MMP1 was maintained in exosomes and exosomal α6β4- and MT1-MMP1–associated C4.4A but not shed C4.4A sufficient for laminin degradation. Hypoxia-induced recruitment of α6β4 toward raft-located C4.4A, MT1-MMP, and TACE allows for a shift from adhesion to motility, which is supported by laminin degradation. These findings provide the first explanation for the C4.4A contribution to wound healing and metastasis.

Neoplasia (2012) 14, 95–107

Introduction

C4.4A is a glycosyl-phosphatidyl-inositol–anchored molecule and belongs, like the urokinase-type plasminogen activator receptor (uPAR), to the Ly6 family [1–3]. C4.4A shares with uPAR three-finger protein domains, characterized by three to six *S-S* bridges, which guarantee maintenance of domain structure by stabilizing the hydrophobic nucleus of the protein [4,5]. uPAR has three and C4.4A two strongly hydrophobic three-finger protein domain [6]. C4.4A has 5 to 6 *N*-glycosylation sites close to the second TFP domain and 15 *O*-glycosylation sites in a Ser/Thr–rich region at the C-terminus [7]. C4.4A associates with laminins (LN) 111 and 332 (formerly LN1 and LN5) and galectin-3 [8].

C4.4A expression is restricted to the basal and suprabasal layers of squamous epithelium in nontransformed tissue [1,2,7,9,10], where it becomes upregulated during wound healing [7,10]. High C4.4A expression has been seen in several types of carcinoma like

mammary, renal cell, colorectal [11–13] and most pronounced non–small cell lung cancer [14]. Its expression in other types of cancer, like esophageal cancer becomes regulated during tumor progression [15,16]. C4.4A transcription requires C/EBPβ and is enhanced by JunD or c-Jun [17], which fits to upregulated expression during wound healing [18–22].

We here aimed to shed light on the molecular mechanism of C4.4A activities, which remain elusive, despite C4.4A being consistently associated with tumor progression and wound healing [3]. These two activities of C4.4A are frequently associated with hypoxia [23,24], which initiates a gene transcription program frequently through hypoxia-inducible factor (HIF) [25,26]. Stabilized HIF-1α undergoes nuclear translocation and associates with transcriptional coactivators [27,28]. Because the C4.4A promoter contains three potential HIF-1α response elements (HREs), we first evaluated whether hypoxia-induced HIF-1α may contribute to *C4.4A* transcription and whether hypoxia influences C4.4A activity in wound healing and tumor cell migration. Under hypoxia, C4.4A forms a complex with $\alpha_6\beta_4$ and MMP14 (formerly MT1-MMP), which promotes motility possibly through focalized LN332 degradation.

Materials and Methods

Tumor Lines

The rat tumor lines were BSp73ASML (ASML, C4.4A$^+$, $\alpha_6\beta_4^+$, metastasizing), BSp73AS (AS, C4.4$^-$, $\alpha_6\beta_4^-$, nonmetastasizing) [29], and BSp73AS1B1 (AS1B1, C4.4A cDNA-transfected AS clone, C4.4A$^+$, $\alpha_6\beta_4^-$). The coding sequence of the C4.4A cDNA has been cloned into the pcDNA3 vector with a CMV promoter to drive C4.4A transcription [1]; Progressor (Prog) (C4.4A$^+$ $\alpha_6\beta_4^+$) [30], 804G (LN332 secreting) [31], and the human A431 (LN332 secreting) [32] were maintained in RPMI/10% fetal calf serum (FCS). The human pancreatic cancer lines Capan-2 (metastasizing) [33], Colo357 (metastasizing) [34], 8.18 (weakly metastasizing) (Tumor Bank, German Cancer Research Center, Heidelberg, Germany; personal observations), and BxPC3 (nonmetastasizing) [35] were maintained in RPMI/10% FCS/10 mM Na-pyruvate. Confluent cultures were trypsinized and split. Where indicated, cells were treated with 100 to 200 µM CoCl$_2$ for 6 to 24 hours or maintained at 1% O$_2$ for 6 to 12 hours.

Antibodies, Matrix Proteins, and Inhibitors

Antibodies, matrix proteins, and inhibitors are listed in Table W1.

Vesicle Depletion and Exosome Preparation

Cells were cultured (48 hours) in serum-free medium. Cleared supernatants (2 × 10 minutes at 500*g*, 1 × 20 minutes at 2000*g*, 1 × 30 minutes at 10,000*g*) were centrifuged (90 minutes at 100,000*g*) and washed (phosphate-buffered saline, 90 minutes at 100,000*g*). The supernatant was collected as vesicle-depleted fraction. The pellet (crude exosomes) was suspended in 2.5 M sucrose, overlaid by a continuous sucrose gradient (0.25-2 M), and centrifuged (15 hours at 150,000*g*).

Flow Cytometry

Flow cytometry followed routine procedures. For intracellular staining, cells were fixed and permeabilized. For chloramphenicol acetyltransferase (CAT) assay standardization, cells were cotransfected with the EGFP-C1 plasmid to evaluate transfection efficacy. Cells were analyzed in a FACScan using the Cell Quest analysis program.

Reverse Transcription–Polymerase Chain Reaction

Total RNA preparation followed standard procedures. Primers are listed in Table W2.

C4.4A Promoter Constructs, Mutations, Transfection, and CAT Assay

A 588-bp and a 1.9-kbp C4.4A promoter constructs have been used [17]. Three CGTG HRE sequences of C4.4A at –673 bp (HRE1), –1183 bp (HRE2), and –1557 bp (HRE3) are shown in Table W3. C4.4A sequences were inserted in promoterless pBLCAT3-Basis (pBLCATB3), which contains the CAT gene [36]. Tk promoter-containing pBLCAT2 served as control [37]. Transfection (3 µg of pBLCAT3-C4.4A, 1 µg of EGFP-C1 or 1.75 µg of pBLCAT3-C4.4A, 1.25 µg of p(HA) HIF-1α 401Δ603 [HIF-1α with oxygen-dependent degradation domain deletion], 1 µg of EGFP-C1) was done as described [17]. For the CAT assay [38], lysates were standardized for protein content and transfection efficacy. Thin-layer chromatography was quantitated using BAS-1800II PhosphorImager (Fuji, Dusseldorf, Germany).

Immunoprecipitation, SDS-PAGE, and Western blot

Cell lysates (60 minutes, 4°C, HEPES buffer, 1% Brij96, protease inhibitor cocktail) were centrifuged (13,000*g* for 10 minutes at 4°C), incubated with antibody (overnight), and precipitated with ProteinG Sepharose (1 hour at 4°C). Washed immune complexes were dissolved in Laemmli buffer. Precipitates/lysates were resolved on 10% SDS-PAGE. Proteins were transferred to nitrocellulose membranes (30 V for 12 hours at 4°C); membranes were blocked, blotted with primary and HRP-conjugated secondary antibodies (1 hour at room temperature), and developed with the ECL kit or were stained with Coomassie blue.

Immunofluorescence and Immunohistochemistry

Cells seeded on bovine serum albumin (BSA)–, LN111-, LN332-, or fibronectin (FN)-coated cover slides were fixed; permeabilized; blocked; incubated with primary antibody (60 minutes at 4°C); fluorochrome-conjugated secondary antibody (60 minutes at 4°C); blocked, incubated with a second, dye-labeled primary antibody (60 minutes at 4°C); and washed. Where indicated, cells were removed by EDTA. Cover slides were mounted in Elvanol (Sigma Aldrich, Steinheim, Germany). Shock-frozen skin sections (7 µm) were exposed to primary antibody, biotinylated secondary antibody, and alkaline phosphatase-conjugated avidin-biotin complex solutions. Sections were counter stained with hematoxylin and eosin. Digitized images were generated using a Leica DMRBE microscope (Leica, Wetzlar, Germany), a SPOT CCD camera, and Software SPOT2.1.2 (Sterling Heights, MI).

Adhesion and Migration Assays

Adhesion to coated 96-well plates was determined after 30 and 240 minutes (37°C). Nonadherent cells were removed by washing. Migration was evaluated in Boyden chambers seeding cells in the upper chamber (RPMI/1% BSA) with/without CoCl$_2$ and/or protease inhibitors. The lower chamber, separated by an 8-µm pore size polycarbonate membrane, contained RPMI/1% BSA or LN332 (804G supernatant). In both assays, cells were stained with crystal violet, measuring OD$_{595nm}$ after lysis. Adhesion/migration is presented as percentage input cells. For *in vitro* wound healing, a subconfluent

monolayer was scratched. Wound closure (light microscopy) is presented as percentage reduction of the freshly wounded area.

Rats and Treatment

A 1-cm-diameter full-thickness skin area was excised from the shaved back of 8-week-old BDX rats. At the time of excision, after 4 and 7 days, rats received 100 µg of control IgG or C4.4 in 100 µl of phosphate-buffered saline, perilesionally. Sterile gauze covering the wound was fixed with a whole-body bandage. A 1.5-cm-diameter area, including the wound, excised immediately, after 1, 3, 7, and 10 days, was shock frozen. Animal experiments were government approved (Baden-Wuerttemberg).

Statistics

Values represent the mean ± SD of triplicates and/or three repetitions. $P < .05$ (Student's t test) was considered statistically significant.

Results

Hypoxia-Induced C4.4A Up-regulation

The impact of hypoxia on C4.4A expression was evaluated in two metastatic C4.4A$^+$ rat tumor lines Prog and ASML, in AS1B1 cells

(C4.4A cDNA-transfected AS cells) [1,29], and in human pancreatic tumor lines.

Cells were cultured in the presence of CoCl$_2$, which mimics hypoxic conditions [39]. High C4.4A expression in ASML and Prog cells was increased after 6 hours of 200 µM CoCl$_2$ treatment and increased further during a 12-hour culture period. Culturing in 1% O$_2$ exerted similar effects (data not shown). AS1B1 cells showed a minor insignificant increase only after 12 hours of CoCl$_2$ treatment. AS cells remained C4.4A$^-$ (Figure 1, A and B). Two human pancreatic cancer cell lines, Colo357 and Capan-2, which express C4.4A at a medium to low level, responded to CoCl$_2$ treatment with a dose- and time-dependent increase in C4.4A expression, where a subfraction showed a very high expression after 200 µM CoCl$_2$ treatment. 8.18 cells, which do not express C4.4A, revealed very weak expression in approximately 15% of cells after 12 hours of 200 µM CoCl$_2$ treatment. BxPC3 cells remained C4.4A$^-$ (Figure 1, C and 1D). Thus, hypoxia can contribute to C4.4A protein up-regulation.

HIF-1α Does Not Promote C4.4A Transcription

Under hypoxia, stabilized HIF-1α acts as a transcription factor. Under normoxia, AS, AS1B1, and ASML cells express HIF-1α at a low level. In ASML cells, HIF-1α showed a strong, dose-dependent
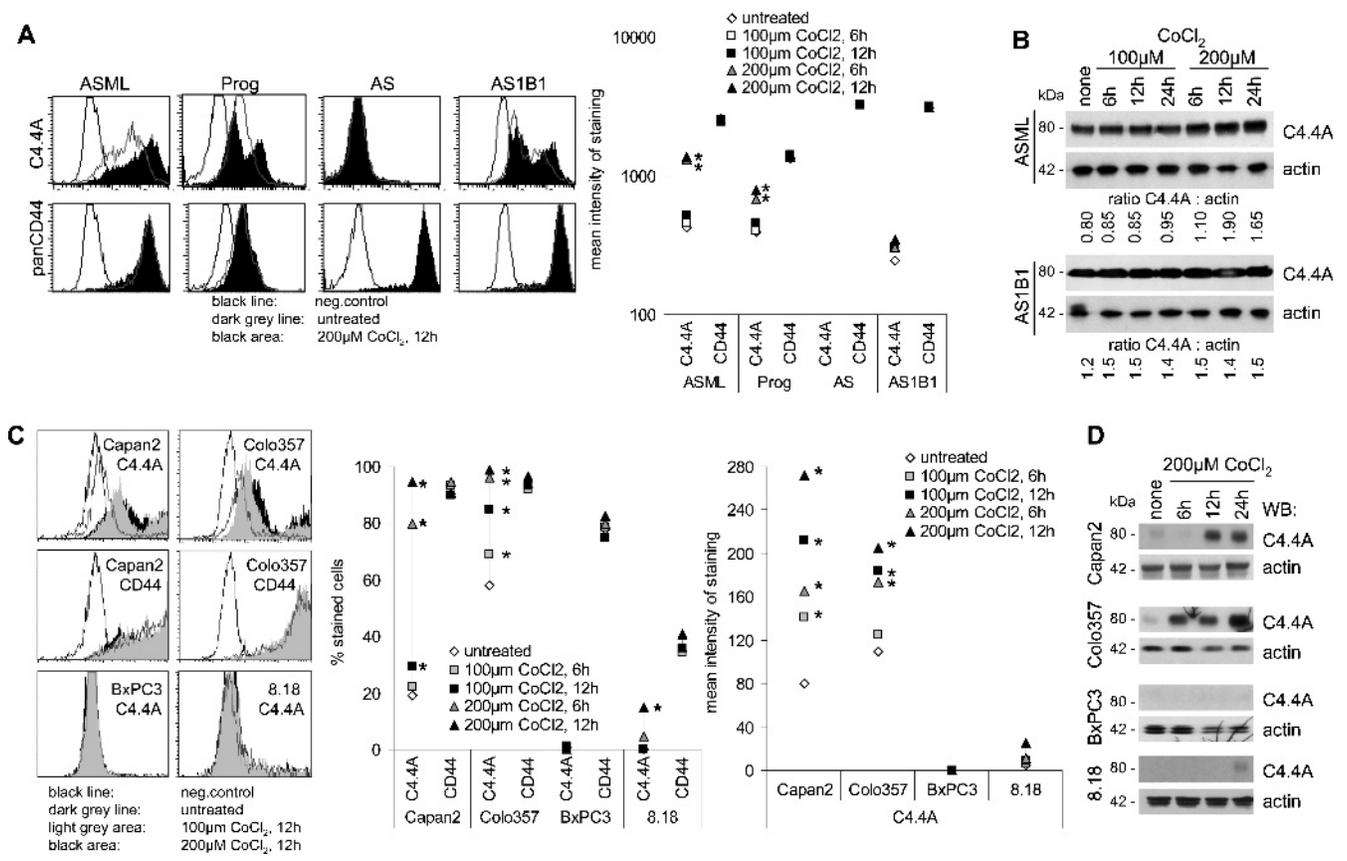
Figure 1. Hypoxia-induced C4.4A up-regulation: (A, B) ASML, Prog, AS, and AS1B1 cells and (C, D) the human pancreatic cancer lines Capan-2, Colo357, BxPC3, and 8.18 were cultured in the presence of titrated amounts of CoCl$_2$ for 6 to 24 hours. (A, C) Expression of C4.4A was evaluated by flow cytometry. Representative examples and (A) mean values of intensity of C4.4A expression or (C) the mean percentage of stained cells and mean intensity in three different experiments is shown. CD44 expression served as control. *Significant differences due to CoCl$_2$ treatment. (B, D) Lysates of untreated and CoCl$_2$-treated cells were separated by SDS-PAGE, transferred and blotted with anti-C4.4A. Actin served as control. In rat and human tumor lines, C4.4A expression increases under hypoxia. C4.4A expression is not or is very weakly induced by hypoxia in cell lines that do not express C4.4A in normoxia.

increase after 12 hours of $CoCl_2$ treatment. Up-regulation was weak after 6 hours and declined beyond 12 hours. An increase in HIF-1α was also seen in $CoCl_2$-treated Capan-2 and BxPC3 cells (Figure 2A). Notably, the latter do not express C4.4A after $CoCl_2$ treatment. This finding suggests that HIF-1α, if at all, may only act as a cotranscription factor for *C4.4A*.

The C4.4A promoter containing three HREs at –673, –1183, and –1557 bp (Table W3), we controlled for HIF-1α cotranscription factor activity in hypoxia. However, when the C4.4A promoter from –588 (no HRE) or from –1957 to –1 bp were inserted into promoterless pBLCAT3, CAT activity of transfected ASML cells, cultured under hypoxia, was not significantly changed (Figure 2B). Furthermore, only a slight increase in CAT activity was observed on cotransfection with pCDNA3-HIF-1α, irrespective of whether the promoter construct contained (1957 bp) or did not contain (588 bp) the three HRE (Figure 2C).
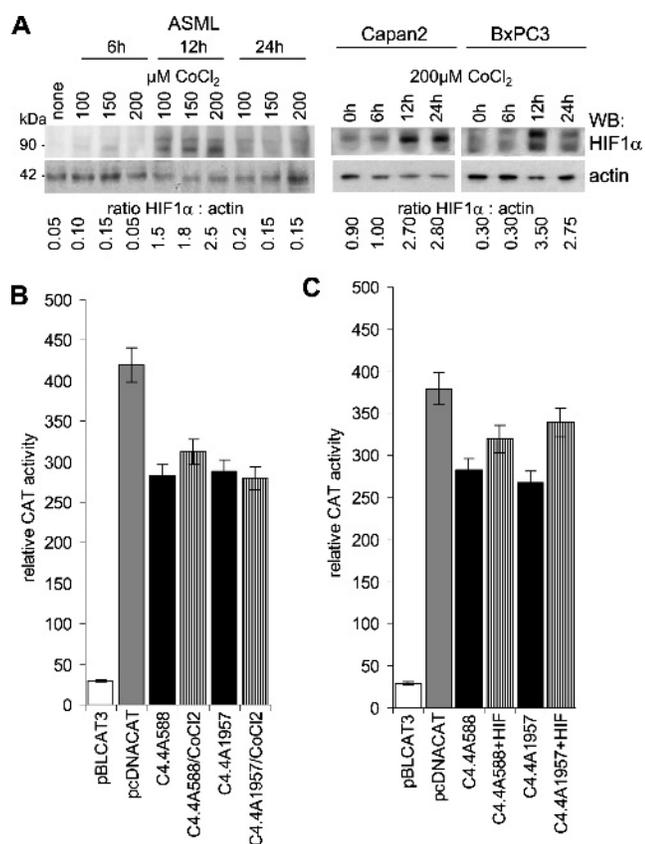
Figure 2. HIF-1α does not promote *C4.4A* transcription: (A) ASML, Capan-2, and BxPC3 cells were cultured in the presence of 200 μM $CoCl_2$ for 6 to 24 hours. HIF-1α expression was evaluated by WB; actin served as control. (B, C) The −1- to −588-bp sequence (no HRE) and the −1- to −1957-bp C4.4A promoter region (three HREs) were cloned into the pBLCAT3 vector. The pcDNA3.1CAT vector (CMV promoter) served as positive; the promoterless pBLCAT3 vector, as negative control. ASML cells were cotransfected with the EGFP-C1 plasmid for standardization. Cells were cultured in the presence or absence of 200 μM $CoCl_2$ for 16 hours. (B) Impact of $CoCl_2$. (C) Impact of HIF-1α as revealed by cotransfection. CAT activity was quantified using a PhosphorImager system. Relative CAT activity (mean ± SD of three experiments) is shown. No significant differences have been seen. Upregulated C4.4A expression under hypoxia may not rely on HIF-1α–induced *C4.4A* transcription.

Thus, hypoxia-induced C4.4A protein up-regulation does, at least, not predominantly proceed at the transcription level.

Hypoxia-Induced C4.4A Up-regulation, LN332 Adhesion, Keratinocyte Migration, and Tumor Cell Motility

Keratinocytes express C4.4A and C4.4A is engaged in wound repair [3,7,8]. Controlling for C4.4A expression and the impact of anti-C4.4A (C4.4) on wound repair after full-thickness skin excision revealed a strong C4.4A expression at the leading front of migrating keratinocytes, and wound closure was strongly delayed in C4.4-treated rats (Figure 3).

With wound repair frequently being associated with hypoxia, we next asked whether hypoxia-induced C4.4A up-regulation affects adhesion or migration on LN332, which, in humans and rats, is a major C4.4A ligand [1,8,10].

ASML, Prog, AS, and AS1B1 cells adhere better to LN332 than BSA. In addition, after 30 minutes, significantly more $CoCl_2$-treated than untreated ASML, Prog, and AS1B1, but not AS cells, adhere to LN332 (Figure 4A). We also evaluated binding to collagen I, III, and IV as well as to FN and vitronectin. Binding did not differ between AS and AS1B1 cells (data not shown), which is in line with the results of pull-down assays that revealed LN332 and (weakly) LN111, but not other matrix, proteins to bind to recombinant C4.4A [8]. Because the increase in binding was more pronounced in ASML and Prog, which both, and distinct to AS, express $\alpha_6\beta_4$, we next asked for the contribution of C4.4A *versus* $\alpha_6\beta_4$ [40] to LN332 adhesion. C4.4 and B5.5 (anti-$\alpha_6\beta_4$) inhibited LN332 binding of untreated and $CoCl_2$-treated ASML and Prog cells with equal efficacy, and no additive inhibitory effect was seen in the presence of both antibodies (data not shown). Binding of $CoCl_2$-treated ASML and Prog cells, but not of AS and AS1B1 cells to BSA, was also slightly inhibited by C4.4 and B5.5, which may be a consequence of both these lines, distinct to AS cells, secreting LN332 [44] (unpublished observations). Binding of AS1B1 cells was only inhibited by C4.4 (Figure 4B).

Because inhibition by C4.4 and B5.5 was stronger in $CoCl_2$-treated cells, we speculated that stress could support joint C4.4A-$\alpha_6\beta_4$ activities. C4.4A and $\alpha_6\beta_4$ did not colocalize in ASML and hardly in Prog cells, when seeded on BSA-coated plates. Weak colocalization was seen in the presence of $CoCl_2$ or on LN332-coated plates. Instead, C4.4A and $\alpha_6\beta_4$ strongly colocalized in $CoCl_2$-treated ASML and Prog cells seeded on LN332 (Figure 4C) and hypoxia strengthened C4.4A-$\alpha_6\beta_4$ coimmunoprecipitation (Figure 4D).

C4.4A-mediated LN332 binding is transient and could be restored in the presence of a protease inhibitor [1]. This also accounts for $CoCl_2$-treated ASML and Prog cells. After 4 hours, adhesion to LN332 did not consistently exceed adhesion to BSA and the adhesion supporting effect of $CoCl_2$ treatment was weak or abolished. Adhesion of $CoCl_2$-treated ASML and Prog cells was partly restored in the presence of broad serine protease (aprotinin) and MMP (MMP-Inh.II) inhibitors. Instead, in C4.4A⁻, $\alpha_6\beta_4^-$ AS cells' adhesion to LN332 was stronger after 4 hours than after 30 minutes. Adhesion was not influenced by $CoCl_2$ and remained unaltered in the presence of MMP-Inh.II. In AS1B1 cells, slightly reduced adhesion to LN332 was at a borderline significant level restored by MMP-Inh.II only in $CoCl_2$-treated cells (Figure 5A). This indicated an essential contribution of C4.4A to reduced LN332 adhesion, which becomes strengthened by $\alpha_6\beta_4$.

As LN332 adhesion decreased with time, hypoxia enhanced migration of ASML and Prog cells on LN332 as revealed by *in vitro* wound healing. Both C4.4 and B5.5 inhibited wound closure of ASML and
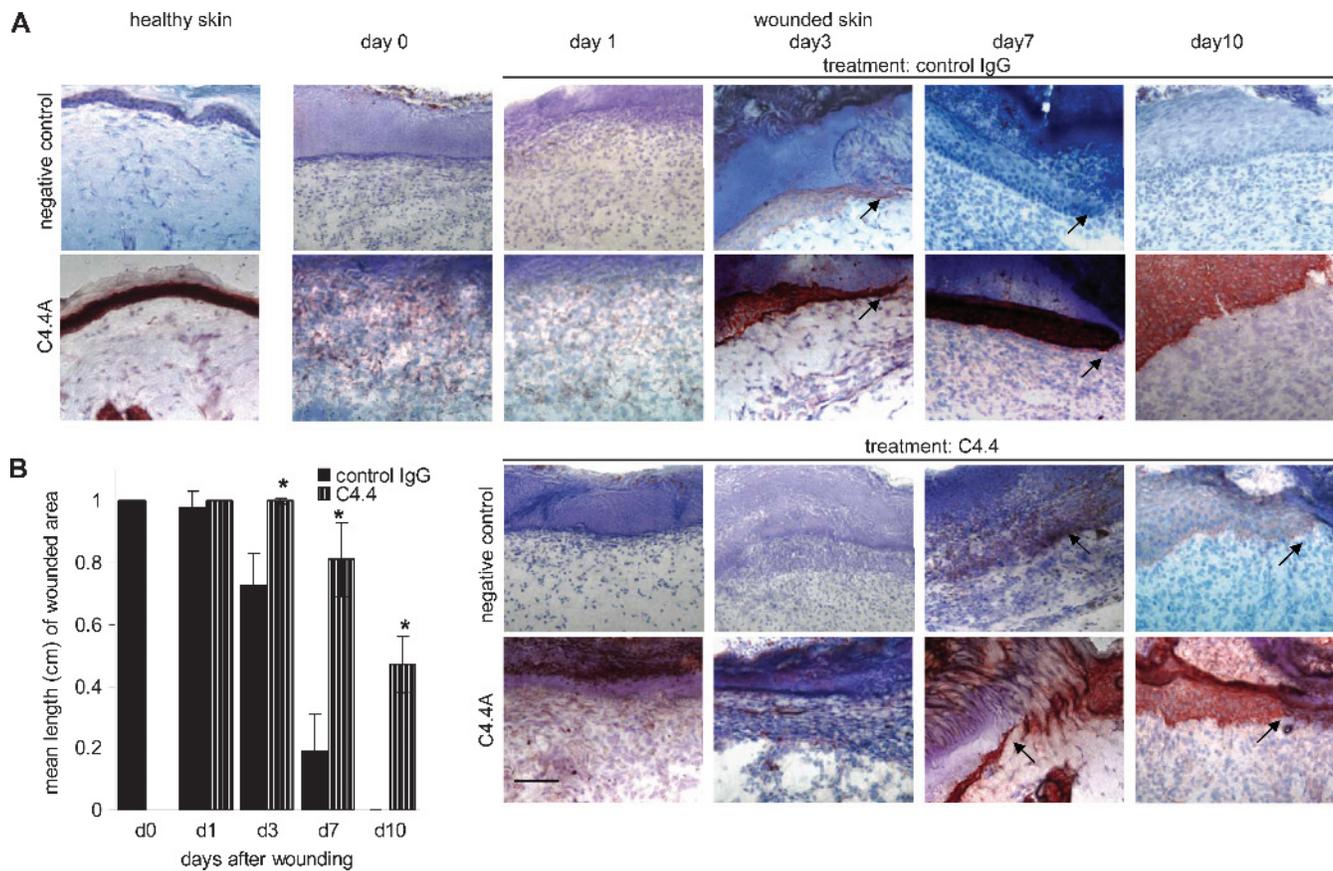
Figure 3. Keratinocyte migration during wound healing and C4.4A expression: The back skin of BDX rats was wounded by a 1-cm-diameter full-thickness skin excision. Rats received at days 0, 4, and 7 after wounding a perilesional injection of 100 μg of control IgG or C4.4. (A) At the time of wounding, after 1, 3, 7, and 10 days, a 1.5-cm area around the wound was excised and shock frozen. Sections (7 μm) were stained with C4.4 or mouse IgG1 (control) and Mayer hematoxylin. Scale bar, 100 μm. Photographs from the wounded skin were obtained from the left side of the wound border. Arrows indicate the migration front of keratinocytes. (B) The mean diameter $\pm$ SD (five rats per group) of the wound area is shown. *Significant differences between control IgG and C4.4-treated wounds. Skin wound healing is accompanied by a high C4.4A expression. C4.4 retards keratinocyte migration.

Prog cells on LN332-coated plates in the presence or absence of CoCl$_2$ (Figure 5B). In line with the MMP-Inh.II–restored adhesiveness to LN332, MMP-Inh.II interfered with migration. MMP-Inh.II exerted no or a minor effect on wound healing of Prog and ASML cells on BSA but significantly inhibited wound healing on LN332 in the presence of CoCl$_2$ (Figure 5C).

Hypoxia-induced increased migratory activity also accounted for transwell migration of ASML and Prog cells, which was promoted by CoCl$_2$ treatment and inhibited by C4.4 and B5.5 (Figure 5D). Transwell migration toward LN332 was inhibited by MMP-Inh.II, although the effect was weak for Prog cells (Figure 5E).

Taken together, hypoxia supports an association of the two LN332 receptors C4.4A and $\alpha_6\beta_4$. Both molecules promote short-term LN332 adhesion but lasting migration. An MMP inhibitor restores adhesiveness and interferes with migration. Thus, hypoxia might be accompanied by increased protease activity accounting for LN332 degradation, where LN332 degradation products can exert chemotactic activity [41–43]. Alternatively, hypoxia might contribute to C4.4A shedding or release.

C4.4A Cooperation with Proteases

ASML [44] and Prog cells secrete LN332. C4.4A poorly colocalized with LN332 on BSA-coated plates under normoxic conditions. Co-

localization was promoted when CoCl$_2$-treated cells were seeded on LN332-coated plates (Figure 6A). Because the experimental setting did not allow to judge on LN332 degradation, ASML and Prog cells were seeded in the presence or absence of CoCl$_2$ on uncoated plates, removing cells after 2 days of culture by EDTA and staining for LN111, LN332, and FN. In CoCl$_2$-treated cultures, the rim staining for LN332 was stronger and more focalized, but the area below the cell body was free of LN332. Instead, FN remained deposited below the cell body independent of CoCl$_2$ treatment. LN111 deposition was reduced but not abolished. Staining of cell-free areas confirmed poor LN332, high FN, and intermediate LN111 recovery (Figure 6B).

These findings argued for LN332 and (partial) LN111 fragmentation. To control the hypothesis, LN111 and LN332 (804G supernatant) were cocultured for 24 hours with ASML cells in the presence of CoCl$_2$ with/without MMP-Inh.II. Cells were removed, and the LNs were separated by SDS-PAGE. Gels were stained with Coomassie blue or proteins were transferred and blotted with anti-LN111 or anti-LNγ2. Coomassie blue staining provided evidence for LN111 and LN332 fragmentation, which was reduced when cultures contained MMP-Inh.II. Western blot (WB) confirmed LNγ2 degradation, and a weaker LN111 band was recovered when LN111 was cocultured with CoCl$_2$-treated ASML cells but not when cultures contained MMP-Inh.II (Figure 6C).
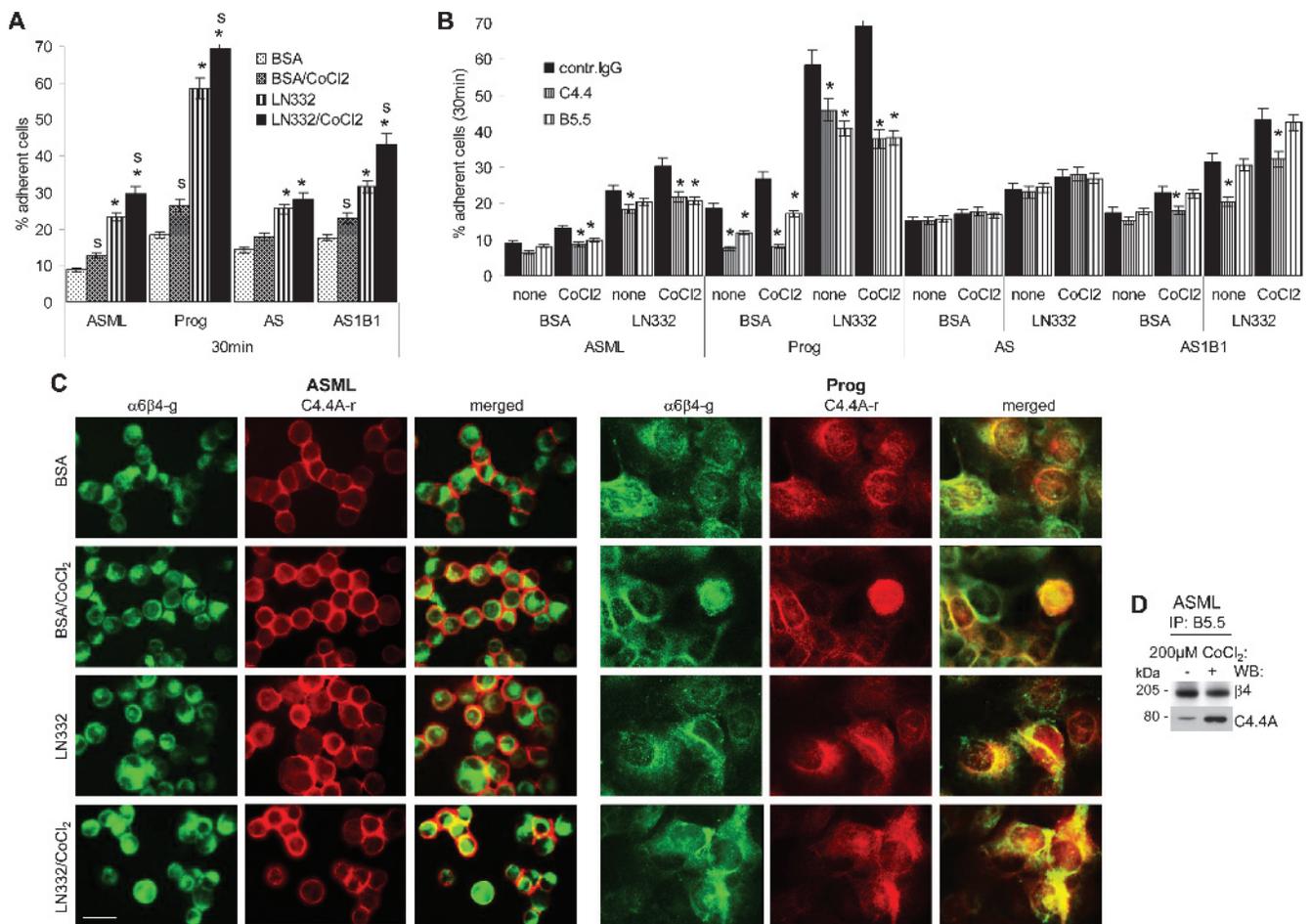
Figure 4. The impact of hypoxia and upregulated C4.4A expression on LN332 adhesion. (A, B) Untreated and CoCl₂-treated ASML, Prog, AS, and AS1B1 cells were seeded on BSA- or 804G supernatant (LN332)–coated plates and cultured for 30 minutes with or without CoCl₂. (B) Cultures contained in addition C4.4 or B5.5 (10 μg/ml). (A, B) The percentage of adherent cells (mean ± SD of triplicates) is shown. (A) *Significant differences between BSA and LN5. ˢSignificant difference of untreated *versus* CoCl₂-treated cells. (B) *Significant antibody inhibition. (C) ASML and Prog cells were cultured on 804G supernatant (LN332)–coated cover slides with or without CoCl₂. Fixed cells were stained with B5.5/anti-mouse IgG-Cy2 and, after blocking, with C4.4-TxR. Single fluorescence staining and digital overlays are shown. Scale bar, 10 μm. (D) ASML cells were cultured for 16 hours with or without CoCl₂. Lysates were immunoprecipitated with B5.5. After SDS-PAGE and protein transfer, membranes were blotted with C4.4 and anti-β4. Hypoxia increases LN332 adhesion, which is equally well inhibited by C4.4 and B5.5, indicating that LN332 adhesion might pursue by a C4.4A-α₆β₄ complex, which is in line with the colocalization and coimmunoprecipitation of the two molecules.

Figure 5. The impact of protease inhibitors on adhesion to and migration on LN332: (A) Untreated and CoCl₂-treated ASML and Prog cells were seeded on BSA- or 804G supernatant (LN332)–coated plates. Where indicated, cultures contained CoCl₂ and/or aprotinin or MMP-Inh.II. Adhesion was measured after 4 hours. The percentage of adherent cells (mean ± SD of triplicates) is shown. (B, C) Subconfluent monolayers of ASML and Prog cells on BSA- or 804G supernatant (LN332)–coated plates were scratched, and wound closure was controlled in the presence or absence of CoCl₂ for 48 or 72 hours. In C, cultures contained MMP-Inh.II. Wound closure was controlled using an inverted microscope. Representative images (B and C: scale bar, 50 μm) and the mean ± SD (triplicates) of wound closure are shown. (D, E) Cells were seeded in Boyden chambers, the lower chamber contained RPMI/1% BSA or 804G supernatant (LN332). (D) Cells were preincubated with C4.4, B5.5, or mouse IgG1. (E) Cultures contained DMSO or MMP-Inh.II. Migration was evaluated after 16 hours. The mean ± SD (triplicates) of transwell migrating cells is shown. (A-D) *Significant differences between BSA and 804G supernatant (LN332). ˢSignificant difference of untreated *versus* CoCl₂-treated cells. For antibody (B, D) and MMP-Inh.II inhibition (A, C, E), *P* values are shown. Hypoxia-only transiently increases LN332 adhesion but strongly promotes migration of C4.4A⁺ cells on LN332, which can be inhibited by C4.4, B5.5, and MMP-Inh.II. This suggests, besides an involvement of the C4.4A-α₆β₄ complex in adhesion/migration, provision of a migratory stimulus by LN332 fragmentation.
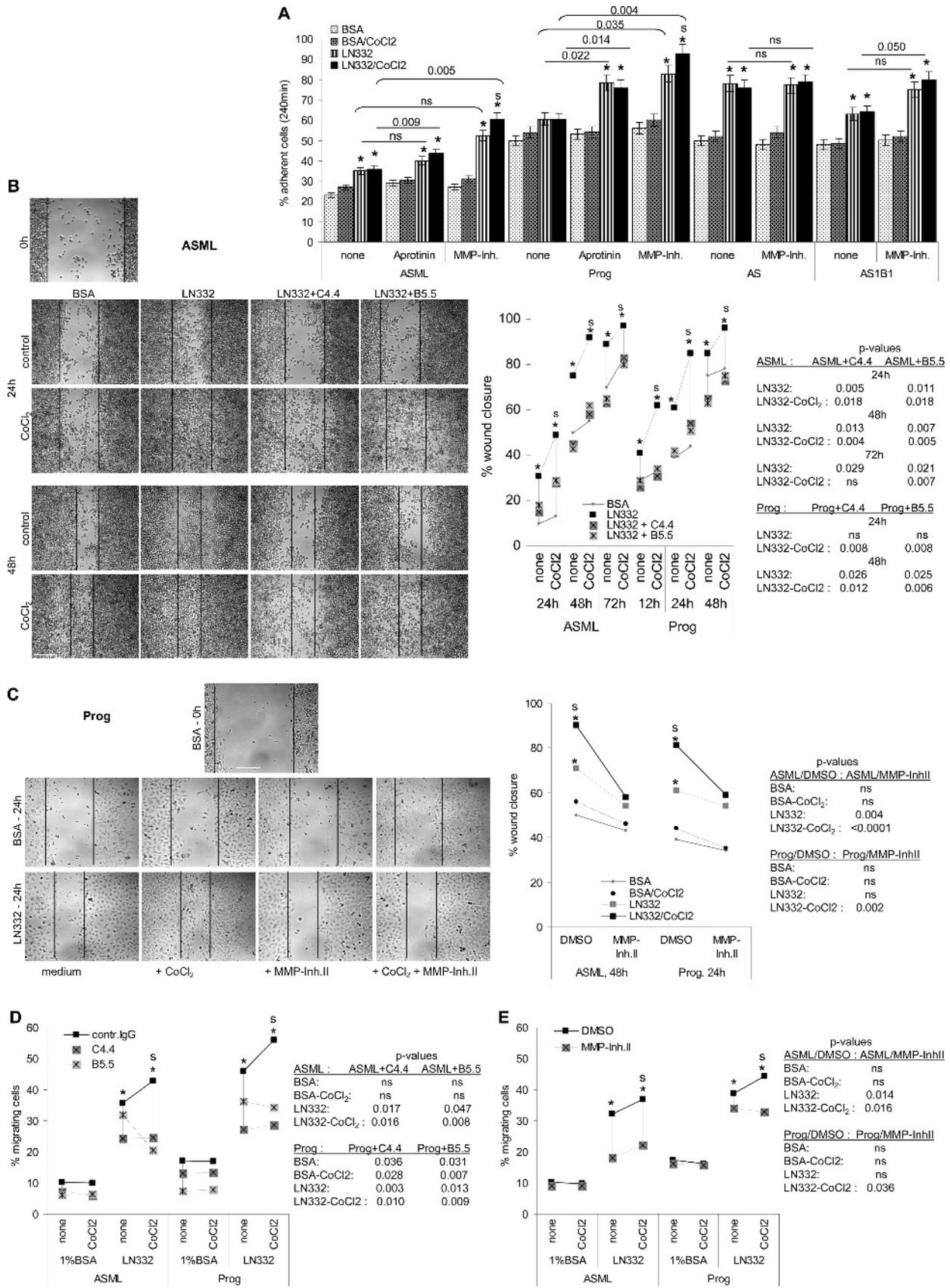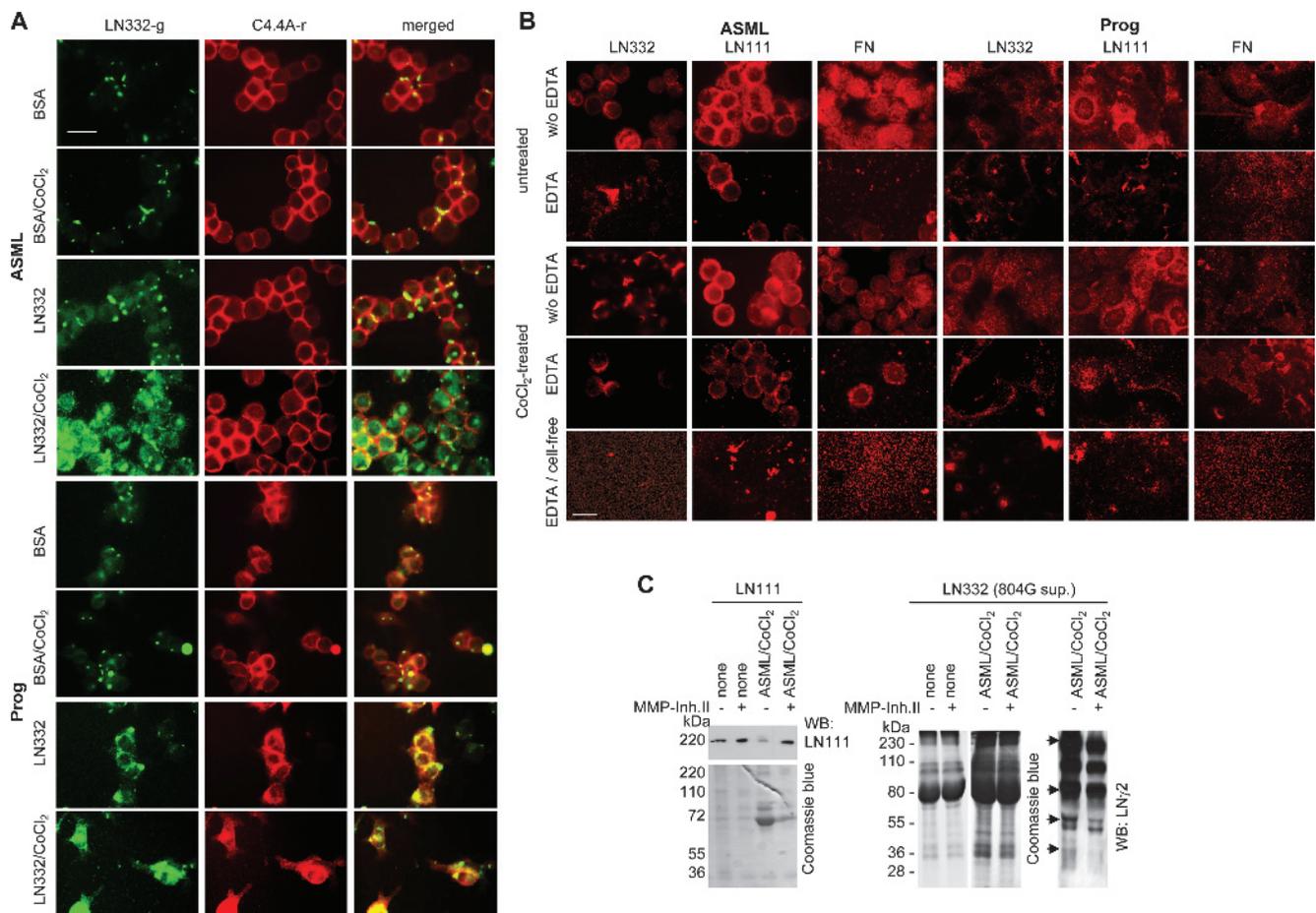
Figure 6. Cooperation of C4.4A and MMP14 in LN332 degradation. (A) ASML and Prog cells cultured on 804G supernatant (LN332)–coated cover slides with or without $CoCl_2$ were fixed and stained with anti-LNγ2/anti–mouse-Cy2 and C4.4-TxR. Single fluorescence and digital overlays are shown. (B) ASML and Prog cells were cultured with or without $CoCl_2$ on glass slides. Cells, cell ghosts (EDTA), and areas, where cells apparently were removed completely ("cell-free" area), were stained with anti-LNγ2, anti-LN111, anti-FN, and Cy3-labeled secondary antibodies. Single fluorescence staining is shown. Scale bar, 5 μm. (C) ASML cells were suspended in 25 μg of LN111 or 250 μg of 804G supernatant (LN332). Cells were incubated at 37°C for 16 hours in the presence of $CoCl_2$ with or without MMP-Inh.II. Cells were removed, and supernatants were dried, dissolved in lysis buffer, and separated by SDS-PAGE. Gels were stained with Coomassie blue or, after transfer, blotted with anti-rat LN111 or anti-rat LNγ2. Hypoxia strengthens C4.4A colocalization with LN332 and supports LN111 and LN332 but not FN fragmentation. MMP-Inh.II inhibits LN degradation.

Thus, C4.4A might promote motility through associated proteases involved in LN degradation. According to the inhibitory activity of MMP-Inh.II, MMP14 was considered a possible candidate. Weak colocalization of MMP14 with C4.4A and $\alpha_6\beta_4$ in resting cells became strong when $CoCl_2$-treated cells were grown on LN332-coated slides (Figure 7A), which corresponded to an increase in coimmunoprecipitation of C4.4A and $\alpha_6\beta_4$ with MMP14 in $CoCl_2$-treated ASML cells. C4.4A and more pronounced $\alpha_6\beta_4$ also coimmunoprecipitated TACE, but not uPA, uPAR, MMP2, and MMP9. Although the C4.4A and $\alpha_6\beta_4$ association with TACE was $CoCl_2$ treatment independent, TACE clustering was more pronounced in $CoCl_2$-treated ASML cells (Figure 7, B-D).

The association of C4.4A with TACE, possibly through $\alpha_6\beta_4$, and the fact that C4.4A has a highly sensitive cleavage site [45] and is delivered in exosomes [8] prompted us to evaluate whether $CoCl_2$ treatment supports C4.4A cleavage and/or exosomal release. C4.4A is recovered in exosomes, a higher amount being recovered from $CoCl_2$-treated cells. Shed C4.4A is only recovered in the supernatant of $CoCl_2$-treated ASML cells. C4.4A shedding is largely abolished in the presence of the

TACE inhibitor (TAPI). However, TAPI did not influence the delivery in exosomes. Exosomal C4.4A and $\alpha_6\beta_4$ also coimmunoprecipitate with MMP14 and TACE (Figure 7E).

These findings raised the question whether exosomal or shed C4.4A would contribute to LN degradation. When exosomes and supernatant from $CoCl_2$-treated ASML cells were coincubated with LN111 and LN332, exosomes, but not shed C4.4A, partly degraded LN111 and LN332. LN degradation by exosomes was also inhibited by MMP-Inh.II (Figure 7F). The experiment was repeated with hLN332, which confirmed partial degradation by Colo357-derived exosomes and inhibition of degradation by MMP-Inh.II. Blot analysis with anti-LNα3, -β3, and -γ2 provided evidence for partial degradation of all three LN332 chains (Figure 7G).

Taken together, hypoxia strengthens C4.4A expression and promotes migration on LN111 and LN332. Migration is accompanied by $\alpha_6\beta_4$ and MMP14 recruitment toward C4.4A and focalized LN5 fragmentation. Owing to the high recovery of C4.4A- and $\alpha_6\beta_4$-associated MMP14 in exosomes, the process of focalized LN332 degradation can also proceed in the surrounding tissue.

Discussion

The function of metastasis-associated C4.4A, with very restricted expression in normal tissue [1,2,7,9,10], remains elusive [3]. We here report that hypoxia-induced C4.4A up-regulation promotes transition from a sessile toward a mobile phenotype through associating with $\alpha_6\beta_4$ and proteases, which supports focalized matrix degrada-

tion. The process is strengthened by the release of C4.4A, $\alpha_6\beta_4$, and MMP14 into exosomes.

Regulation of C4.4A Expression in Hypoxia

Low oxygen and, as a surrogate, $CoCl_2$ treatment [39] are accompanied by HIF-1α transport to the nucleus, where it acts as a transcription
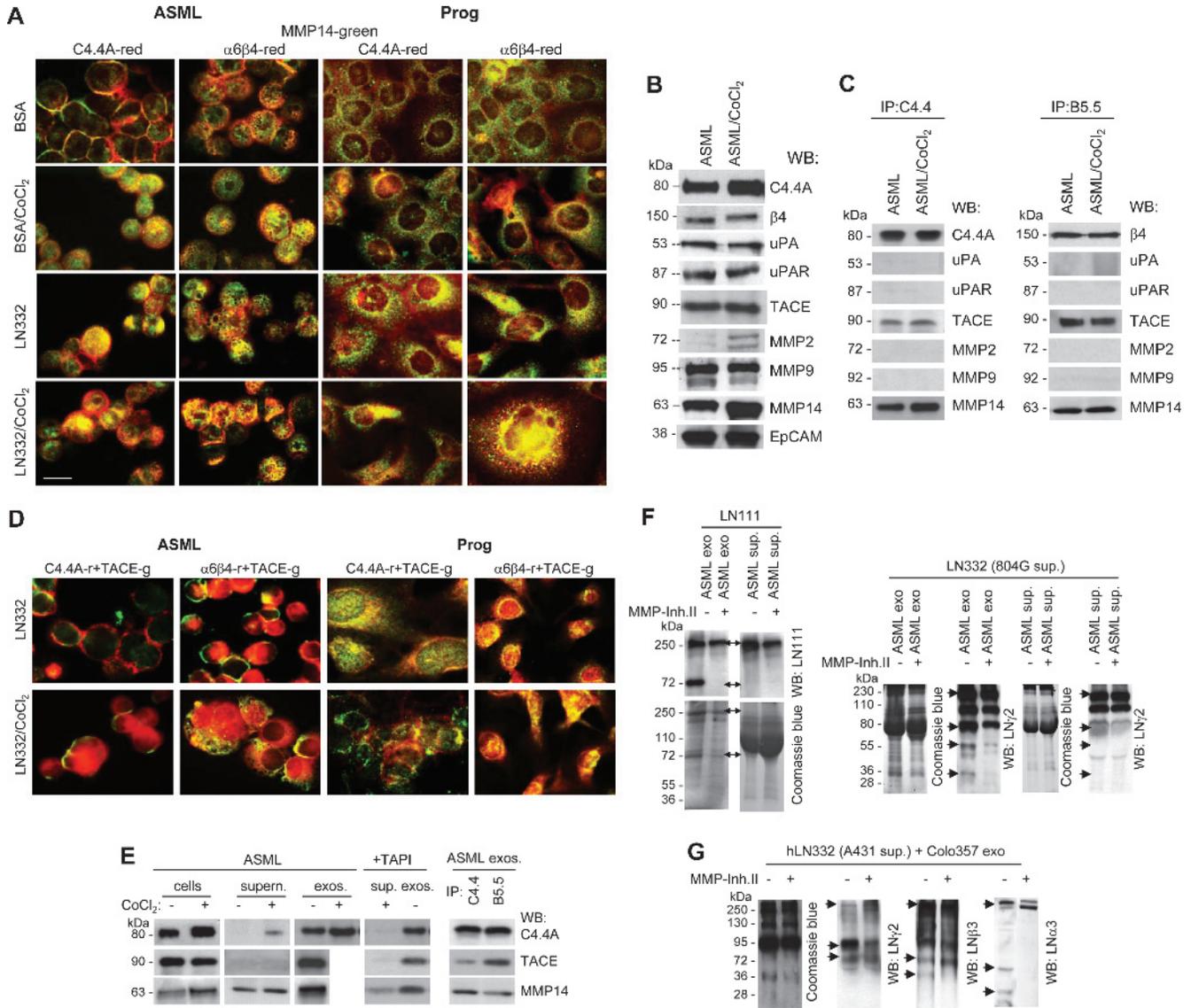
Figure 7. The C4.4A association with proteases, C4.4A shedding, and exosome inclusion in hypoxia. (A) ASML and Prog, grown on BSA- or 804G supernatant (LN332)–coated plates in the presence or absence of $CoCl_2$, were stained with anti–MMP14/anti–rabbit-Cy2 and C4.4-TxR or B5.5-TxR. Digital overlays are presented. Scale bar, 5 μm. (B) Expression of C4.4A, $\alpha_6\beta_4$, uPA, uPAR, TACE, MMP2, MMP9, and MMP14 in untreated and $CoCl_2$-treated ASML cells. (C) Coimmunoprecipitation of C4.4A and $\alpha_6\beta_4$ with uPAR, TACE, MMP2, MMP9, and MMP14. (D) Colocalization of C4.4A and $\alpha_6\beta_4$ with TACE in untreated and $CoCl_2$-treated ASML and Prog grown on 804G supernatant (LN332)–coated glass slides. Digital overlays of staining with anti–TACE/anti–rabbit-Cy2 and C4.4-TxR or B5.5-TxR are shown. Scale bar, 5 μm. (E) ASML cells were cultured in the absence of FCS with or without $CoCl_2$ and TAPI. Vesicle-depleted supernatant and lysed exosomes (20 μg) were separated by SDS-PAGE, transferred, and blotted with C4.4, anti-MMP14, and anti-TACE. Precipitates of exosome lysates with C4.4 and B5.5 were separated by SDS-PAGE and, after transfer, blotted with C4.4, anti–MMP14, and anti-TACE. (F, G) Vesicle-depleted supernatant or exosomes of $CoCl_2$-treated ASML and Colo357 cells were incubated with 10 μg/ml LN111 or 50 μg of 804G supernatant (LN332) or 50 μg of A431 supernatant (LN332) in the presence or absence of MMP-Inh.II. After 16 hours of incubation, cultures were dried and proteins were dissolved in lysis buffer. Samples were separated by SDS-PAGE, and gels were stained with Coomassie blue or proteins were transferred and stained with anti-rat LN111, anti-rat LNγ2, anti-human LNα3, anti-human LNβ3, or anti-human LNγ2. C4.4A and $\alpha_6\beta_4$ associate with TACE and MMP14. The latter is promoted by $CoCl_2$ treatment. Only supernatant of $CoCl_2$-treated ASML cells contained shed C4.4A, where TACE contributes to C4.4A shedding. Hypoxia strengthens incorporation of functionally active and associated C4.4A, $\alpha_6\beta_4$, and MMP14 into exosomes, such that LN111 and LN332 become partially degraded by exosomes.
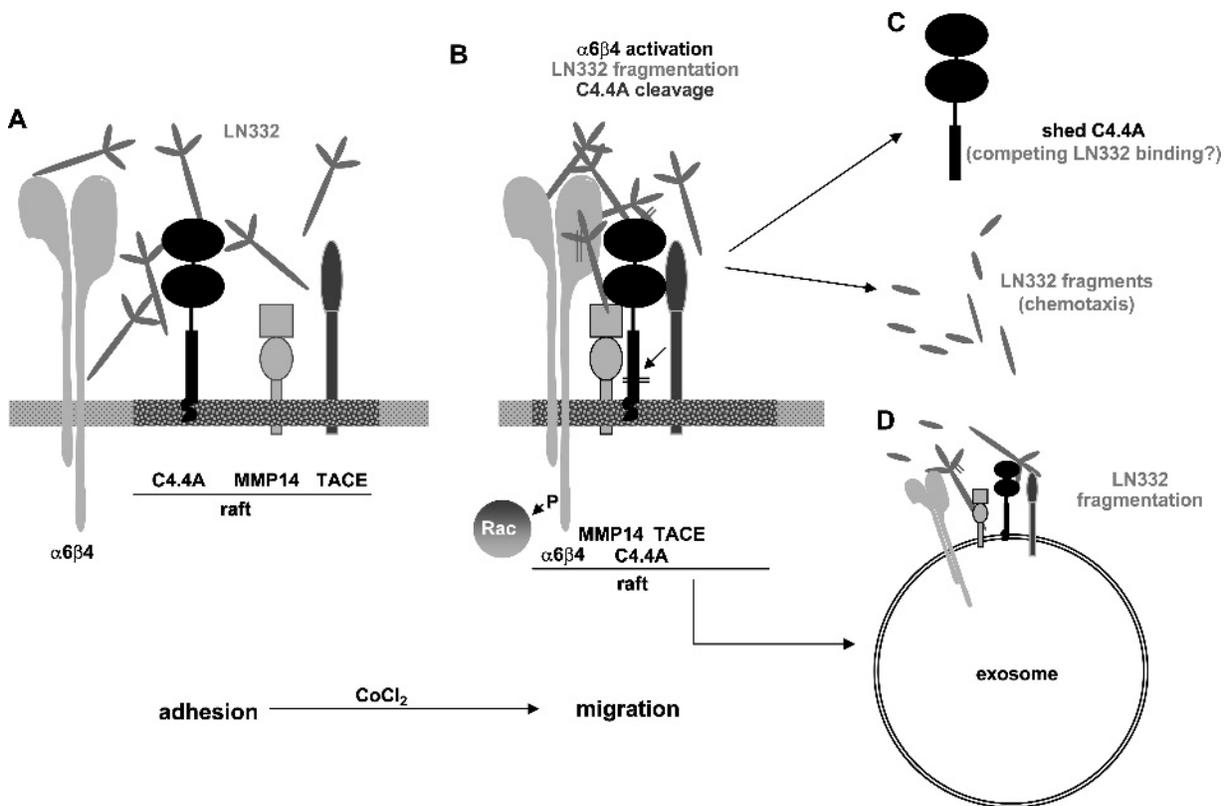
Figure 8. Schematic presentation of C4.4A, $\alpha_6\beta_4$, and protease cooperation in LN migration. (A) C4.4A, MMP14, and TACE are raft located molecules. In resting cells, $\alpha_6\beta_4$ is located outside rafts. Both C4.4A and $\alpha_6\beta_4$ are LN receptors. (B) By binding to LN332 and supported by hypoxia, $\alpha_6\beta_4$ becomes activated and possibly through the joint LN ligand with C4.4A recruited into rafts. Within rafts, activated β_4 initiates rac activation and thereby motility and C4.4A- and $\alpha_6\beta_4$-associated MMP14 becomes activated and contributes to LN degradation. In addition, C4.4A becomes cleaved by TACE. (C) Defined LN5 degradation products can act as chemoattractant, which further supports motility. Whether shed C4.4A competes for LN binding has not been explored. (D) In activated cells, raft-located proteins are prone for internalization and, after recruitment into multivesicular bodies, for release in exosomes. Accordingly, C4.4A- and $\alpha_6\beta_4$-associated MMP14 are recovered in exosomes, such that exosomal MMP14 further contributes to LN degradation. C4.4A is also recovered in vesicle-free culture supernatant, which is due to C4.4A cleavage by TACE.

factor for multiple genes [26,28]. Because hypoxia is accompanied by upregulated C4.4A expression and the *C4.4A* promoter contains three HREs, we considered the possibility that HIF-1α may contribute to *C4.4A* transcription. However, cotransfection with HIF-1α did not show an HIF-1α contribution to *C4.4A* transcription. C/EBPβ, essentially required for C4.4A transcription [17], has also been associated with metastasis-associated gene transcription [46], gene expression in differentiating keratinocytes, and wound repair [47,48]. However, although a high CAT activity was observed after cotransfection with C/EBPβ, we did not observe a further increase by CoCl$_2$ treatment (data not shown). Thus, high C4.4A expression under hypoxia may be a consequence of protein stabilization. The finding that CoCl$_2$ treatment did not induce expression in C4.4A-negative tumor lines is in line with this interpretation.

Cooperation of C4.4A with $\alpha_6\beta_4$ and MMP14

C4.4A is strongly expressed in migrating keratinocytes during wound repair where a direct contribution to keratinocyte migration has been demonstrated by C4.4, significantly inhibiting wound healing. *In vitro*, CoCl$_2$ treatment promoted migration of C4.4A$^+$ tumor cells on LN332, a major C4.4A ligand [8], after a transient increase in LN332 adhesion.

The engagement of C4.4A in the shift toward motility on LN332 could rely on hypoxia-induced associations of C4.4A with $\alpha_6\beta_4$ and MMP14. On LN332, but not on BSA, C4.4A colocalizes and associates with $\alpha_6\beta_4$, with focalized colocalization and association being stronger under hypoxia. ASML, Prog, and AS/AS1B1 also express $\alpha_3\beta_1$ and $\alpha_6\beta_1$. However, neither of these integrins coimmunoprecipitated C4.4A in resting cells or in stimulated cells. Thus, it is the association between C4.4A and $\alpha_6\beta_4$ that has bearing on adhesion/migration of ASML and Prog cells. LN332 is a major ligand for $\alpha_6\beta_4$ [40,49], and one could have speculated that C4.4A only acts as an accessory molecule. This has been excluded because recombinant C4.4A binds LN332 [8] and AS1B1 cells, which do not express $\alpha_6\beta_4$ [1], also showing pronounced LN332 binding. However, the effect of C4.4A by itself as demonstrated in AS1B1 cells on LN332 binding and motility (data not shown) is much weaker than in cells, where C4.4A associates with $\alpha_6\beta_4$ in hypoxia (ASML, Prog). In line with this finding, adhesion and migration on LN332 became equally well inhibited by C4.4 and anti-$\alpha_6\beta_4$.

Pronounced adhesion of ASML and Prog cells to LN332 is transient. It is known that $\alpha_6\beta_4$ contributes to tumor cell motility [49–54] that can be initiated through binding of $\alpha_6\beta_4$ to LN332. Furthermore, $\alpha_6\beta_4$ becomes recruited toward rafts in stimulatory conditions [55,56]. This is accompanied by phosphorylation of the β_4 cytoplasmic domain [57–59], recruitment of Shc, and activation of downstream signaling

molecules [60] like rac with a central role in directional cell migration [61,62]. Taking this into account, it becomes likely that the joint activity of C4.4A with $\alpha_6\beta_4$ accounts for the shift from adhesion to motility. Whether C4.4A actively recruits $\alpha_6\beta_4$ or whether $\alpha_6\beta_4$ and C4.4A come into vicinity through their joint ligand(s) remains to be explored.

Finally, proteolytic processing of LN332 also can support cell migration [63]. The rat $\gamma2$ chain can be cleaved by MMP2 and MMP14 [42]. One of the $\gamma2$ fragments interacts with and activates the epidermal growth factor receptor [64]. Different LN332 fragments from the $\gamma2$ and the $\alpha3$ chain also account for the deposition into the matrix underlying cultured cells [65,66]. MMP14 and hepsin can also cleave the $\beta3$ chain [43,67], where hepsin cleavage promotes motility on LN332 [67]; the $\alpha3$ chain can be cleaved by several proteases including plasmin [68]. Three observations are in line with hypoxia-induced C4.4A up-regulation and the association with $\alpha_6\beta_4$ accounting for the pronounced migration due to LN332 fragmentation: 1) broad serine or MMP inhibitors promoted LN332 adhesion, 2) LN332 deposits were not recovered in $CoCl_2$-treated cultures, and 3) an MMP inhibitor–reduced migration on LN332. Because aprotinin partially restored adhesion to LN332, but MMP-Inh.II exerted stronger effects on cell migration, we tested several proteases for associating with C4.4A and $\alpha_6\beta_4$. Both LN332 ligands do not associate with uPAR, uPA, MMP2, or MMP9 but associate with TACE and more strongly in hypoxia with MMP14. In addition, rat and human LN332 becomes degraded by $CoCl_2$-treated C4.4A$^+$ and $\alpha_6\beta_4^+$ tumor cells, and a broad MMP inhibitor interferes with degradation. Whether additional proteases like hepsin may also associate with C4.4A and contribute to LN332 degradation [67] remains to be explored.

Thus, the engagement of C4.4A in tissue remodeling, wound repair, and tumor progression may well rely on its hypoxia-induced association with $\alpha_6\beta_4$ and MMP14.

Hypoxia and C4.4A Release

C4.4A shedding and exosomal release [11] are both stimulated by hypoxia. The increase in soluble C4.4A could be linked to TACE that cleaves C4.4A [69]. Using SILAC (stable isotope labeling by amino acids in cell culture), the authors demonstrate in a human mammary carcinoma line that C4.4A is a new substrate for both ADAM10 and ADAM17/TACE and speculate that cleavage of C4.4A by ADAM10 and TACE may contribute to tumor progression [69]. Our findings of coimmunoprecipitation of C4.4A and $\alpha_6\beta_4$ with TACE, the increased recovery of C4.4A in vesicle-free culture supernatant, and the inhibition of C4.4A release by TAPI are fully in line with the described findings and support the authors' interpretation that the C4.4A-TACE association may contribute to metastasizing tumor cell motility. The increase in exosomal C4.4A corresponds to a pronounced exosome release under stress [70]. In line with the internalization of membrane microdomains, such that internalized protein complexes remain intact [71], exosomes collected from $CoCl_2$-treated tumor cells contained C4.4A, $\alpha_6\beta_4$, and MMP14, where, for the latter, clathrin- and caveolin-dependent internalization has been described [72]. Importantly, the exosomal $\alpha_6\beta_4$- and MMP14-associated C4.4A, but not soluble C4.4A, supports LN332 degradation. This confirms that not C4.4A by itself but a complex of C4.4A and $\alpha_6\beta_4$ with proteases is required for LN fragmentation. Exosomal proteins are functionally active [73], which also accounts for MMP14 [74]. Accordingly, the activity of the C4.4A- and $\alpha_6\beta_4$-associated MMP14 is not restricted to the cell membrane but can additionally prepare the surrounding of migrating epithelial and tumor cells, thus extending the operational range of C4.4A.

Conclusions

As summarized in Figure 8, hypoxia-induced C4.4A up-regulation is accompanied, after a transient increase in LN adhesion, by pronounced migration, where migration on LN depends on the association of C4.4A with $\alpha_6\beta_4$ under hypoxia. C4.4A- and $\alpha_6\beta_4$-associated MMP14 could contribute to the shift toward migration by facilitating focalized LN degradation. Importantly, hypoxia also strengthens the release of exosomes, which express C4.4A- and $\alpha_6\beta_4$-associated MMP14. Exosomes thus expand the range of functional activity of C4.4A in wound healing, tissue remodeling, and tumor cell spread.

Acknowledgments

References

[1] Rösel M, Claas C, Seiter S, Herlevsen M, and Zöller M (1998). Cloning and functional characterization of a new phosphatidyl-inositol anchored molecule of a metastasizing rat pancreatic tumor. *Oncogene* **17**, 1989–2002.

[2] Würfel J, Rösel M, Seiter S, Claas C, Herlevsen M, Weth R, and Zöller M (2001). Cloning of the human homologue of the metastasis-associated rat C4.4A. *Gene* **262**, 35–41.

[3] Jacobsen B and Ploug M (2008). The urokinase receptor and its structural homologue C4.4A in human cancer: expression, prognosis and pharmacological inhibition. *Curr Med Chem* **15**, 2559–2573.

[4] Tsetlin V (1999). Snake venom α-neurotoxins and other "three-finger" proteins. *Eur J Biochem* **264**, 281–286.

[5] Fry BG (2005). From genome to "venome": molecular origin and evolution of the snake venom proteome inferred from phylogenetic analysis of toxin sequences and related body proteins. *Genome Res* **15**, 403–420.

[6] Galat A (2008). The three-fingered protein domain of the human genome. *Cell Mol Life Sci* **65**, 3481–3493.

[7] Hansen LV, Gardsvoll H, Nielsen BS, Lund LR, Jensen ON, and Ploug M (2004). Structural analysis and tissue localization of human C4.4A: a protein homologue of the urokinase receptor. *Biochem J* **380**, 845–857.

[8] Paret C, Bourouba M, Beer A, Miyazaki K, Schnölzer M, Fiedler S, and Zöller M (2005). Ly6 family member C4.4A binds laminins 1 and 5 associates with galectin-3 and supports cell migration. *Int J Cancer* **115**, 724–733.

[9] Claas C, Herrmann K, Matzku S, Möller P, and Zöller M (1996). Developmentally regulated expression of metastasis-associated antigens in the rat. *Cell Growth Differ* **7**, 663–678.

[10] Smith BA, Kennedy WJ, Harnden P, Selby PJ, Trejdosiewicz LK, and Southgate J (2001). Identification of genes involved in human urothelial cell-matrix interactions: implications for the progression pathways of malignant urothelium. *Cancer Res* **61**, 1678–1685.

[11] Paret C, Hildebrand D, Weitz J, Kopp-Schneider A, Kuhn A, Beer A, Hautmann R, and Zöller M (2007). C4.4A as a candidate marker in the diagnosis of colorectal cancer. *Br J Cancer* **97**, 1146–1156.

[12] Seiter S, Stassar M, Rappl G, Reinhold U, Tilgen W, and Zöller M (2001). Upregulation of C4.4A expression during progression of melanoma. *J Invest Dermatol* **116**, 344–347.

[13] Fletcher GC, Patel S, Tyson K, Adam PJ, Schenker M, Loader JA, Daviet L, Legrain P, Parekh R, Harris AL, et al. (2003). hAG-2 and hAG-3 human homologues of genes involved in differentiation are associated with oestrogen receptor–positive breast tumours and interact with metastasis gene *C4.4a* and dystroglycan. *Br J Cancer* **88**, 579–585.

[14] Hansen LV, Skov BG, Ploug M, and Pappot H (2007). Tumour cell expression of C4.4A, a structural homologue of the urokinase receptor, correlates with poor prognosis in non–small cell lung cancer. *Lung Cancer* **58**, 260–266.

[15] Hansen LV, Laerum OD, Illemann M, Nielsen BS, and Ploug M (2008). Altered expression of the urokinase receptor homologue, C4.4A, in invasive areas of human esophageal squamous cell carcinoma. *Int J Cancer* **122**, 734–741.

[16] Wang W, Ding YQ, Li ZG, Han HX, and Yang L (2006). Expression and diagnostic application of C4.4A protein in squamous cell carcinoma and adenocarcinoma [in Chinese]. *Zhonghua Bing Li Xue Za Zhi* **35**, 277–280.

[17] Fries F, Nazarenko I, Hess J, Claas A, Angel P, and Zöller M (2007). CEBPβ, JunD and c-Jun contribute to the transcriptional activation of the metastasis-associated *C4.4A* gene. *Int J Cancer* **120**, 2135–2147.

[18] Meir O, Dvash E, Werman A, and Rubinstein M (2010). C/EBP-β regulates endoplasmic reticulum stress–triggered cell death in mouse and human models. *PLoS One* **5**, e9516.

[19] Staiger J, Lueben MJ, Berrigan D, Malik R, Perkins SN, Hursting SD, and Johnson PF (2009). C/EBPβ regulates body composition, energy balance–related hormones and tumor growth. *Carcinogenesis* **30**, 832–840.

[20] Kirstetter P, Schuster MB, Bereshchenko O, Moore S, Dvinge H, Kurz E, Theilgaard-Mönch K, Månsson R, Pedersen TA, Pabst T, et al. (2008). Modeling of C/EBPα mutant acute myeloid leukemia reveals a common expression signature of committed myeloid leukemia-initiating cells. *Cancer Cell* **13**, 299–310.

[21] Franco-Montoya ML, Bourbon JR, Durrmeyer X, Lorotte S, Jarreau PH, and Delacourt C (2009). Pulmonary effects of keratinocyte growth factor in newborn rats exposed to hyperoxia. *Am J Physiol Lung Cell Mol Physiol* **297**, L965–L976.

[22] Koria P and Andreadis ST (2007). KGF promotes integrin α_5 expression through CCAAT/enhancer–binding protein-β. *Am J Physiol Cell Physiol* **293**, C1020–C1031.

[23] Tandara AA and Mustoe TA (2004). Oxygen in wound healing—more than a nutrient. *World J Surg* **28**, 294–300.

[24] Finger EC and Giaccia AJ (2010). Hypoxia, inflammation, and the tumor microenvironment in metastatic disease. *Cancer Metastasis Rev* **29**, 285–293.

[25] Fitsialos G, Bourget I, Augier S, Ginouvès A, Rezzonico R, Odorisio T, Cianfarani F, Virolle T, Pouysségur J, Meneguzzi G, et al. (2008). HIF1 transcription factor regulates laminin-332 expression and keratinocyte migration. *J Cell Sci* **121**, 2992–3001.

[26] Yee Koh M, Spivak-Kroizman TR, and Powis G (2008). HIF-1 regulation: not so easy come, easy go. *Trends Biochem Sci* **33**, 526–534.

[27] Kaluz S, Kaluzová M, and Stanbridge EJ (2008). Regulation of gene expression by hypoxia: integration of the HIF-transduced hypoxic signal at the hypoxia-responsive element. *Clin Chim Acta* **395**, 6–13.

[28] Brahimi-Horn MC and Pouysségur J (2009). HIF at a glance. *J Cell Sci* **122**, 1055–1057.

[29] Matzku S, Komitowski D, Mildenberger M, and Zöller M (1983). Characterization of BSp73 a spontaneous rat tumor and its *in vivo* selected variants showing different metastasizing capacities. *Invasion Metastasis* **3**, 109–123.

[30] Martin F, Caignard A, Jeannin JF, Leclerc A, and Martin M (1983). Selection by trypsin of two sublines of rat colon cancer cells forming progressive or regressive tumors. *Int J Cancer* **32**, 623–627.

[31] Homma Y, Ozono S, Numata I, Seidenfeld J, and Oyasu R (1985). α-Difluoromethylornithine inhibits cell growth stimulated by a tumor-promoting rat urinary fraction. *Carcinogenesis* **6**, 159–161.

[32] Panneerselvam M, Sahai A, and Salomon DS (1985). Modulation of type-IV procollagen and laminin production in A431 human squamous epidermoid carcinoma cells by 12-O-tetradecanoylphorbol-13-acetate (TPA) and epidermal growth factor (EGF). *Arch Dermatol Res* **277**, 377–383.

[33] Takamori H, Hiraoka T, and Yamamoto T (1996). Expression of tumor-associated carbohydrate antigens correlates with hepatic metastasis of pancreatic cancer: clinical and experimental studies. *Hepatogastroenterology* **43**, 748–755.

[34] Morgan RT, Woods LK, Moore GE, Quinn LA, McGarvan L, and Gordon SG (1980). Human cell line (COLO 357) of metastatic pancreatic adenocarcinoma. *Int J Cancer* **25**, 591–598.

[35] Tan MH, Nowak NJ, Loor R, Ochi H, Sandberg AA, Lopez C, Pickren JW, Berjian R, Douglass HO Jr, and Chu TM (1986). Characterization of a new primary human pancreatic tumor line. *Cancer Invest* **4**, 15–23.

[36] Luckow B and Schütz G (1987). CAT constructions with multiple unique restriction sites for the functional analysis of eukaryotic promoters and regulatory elements. *Nucleic Acids Res* **15**, 5490.

[37] Burger HJ, Schuetz JD, Schuetz EG, and Guzelian PS (1992). Paradoxical transcriptional activation of rat liver cytochrome P-450 3A1 by dexamethasone and the antiglucocorticoid pregnenolone 16 α-carbonitrile: analysis by transient transfection into primary monolayer cultures of adult rat hepatocytes. *Proc Natl Acad Sci USA* **89**, 2145–2149.

[38] Gorman CM, Moffat LF, and Howard BH (1982). Recombinant genomes which express chloramphenicol acetyltransferase in mammalian cells. *Mol Cell Biol* **2**, 1044–1051.

[39] Liu XH, Kirschenbaum A, Yao S, Stearns ME, Holland JF, Claffey K, and Levine AC (1999). Upregulation of vascular endothelial growth factor by cobalt chloride-simulated hypoxia is mediated by persistent induction of cyclooxygenase-2 in a metastatic human prostate cancer cell line. *Clin Exp Metastasis* **17**, 687–694.

[40] Rabinovitz I and Mercurio AM (1996). The integrin $\alpha_6\beta_4$ and the biology of carcinoma. *Biochem Cell Biol* **74**, 811–821.

[41] Giannelli G, Falk-Marzillier J, Schiraldi O, Stetler-Stevenson WG, and Quaranta V (1997). Induction of cell migration by matrix metalloprotease-2 cleavage of laminin-5. *Science* **277**, 225–228.

[42] Koshikawa N, Giannelli G, Cirulli V, Miyazaki K, and Quaranta V (2000). Role of cell surface metalloprotease MT1-MMP in epithelial cell migration over laminin-5. *J Cell Biol* **148**, 615–624.

[43] Udayakumar TS, Chen ML, Bair EL, Von Bredow DC, Cress AE, Nagle RB, and Bowden GT (2003). Membrane type-1–matrix metalloproteinase expressed by prostate carcinoma cells cleaves human laminin-5 β_3 chain and induces cell migration. *Cancer Res* **63**, 2292–2299.

[44] Jung T, Castellana D, Klingbeil P, Cuesta Hernández I, Vitacolonna M, Orlicky DJ, Roffler SR, Brodt P, and Zöller M (2009). CD44v6 dependence of premetastatic niche preparation by exosomes. *Neoplasia* **11**, 1093–1105.

[45] Gårdsvoll H, Hansen LV, Jørgensen TJ, and Ploug M (2007). A new tagging system for production of recombinant proteins in *Drosophila* S2 cells using the third domain of the urokinase receptor. *Protein Expr Purif* **52**, 384–394.

[46] Chun KS and Surh YJ (2004). Signal transduction pathways regulating cyclooxygenase-2 expression: potential molecular targets for chemoprevention. *Biochem Pharmacol* **68**, 1089–1100.

[47] Maytin EV, Lin JC, Krishnamurthy R, Batchvarova N, Ron D, Mitchell PJ, and Habener JF (1999). Keratin 10 gene expression during differentiation of mouse epidermis requires transcription factors C/EBP and AP-2. *Dev Biol* **216**, 164–181.

[48] House JS, Zhu S, Ranjan R, Linder K, and Smart RC (2010). C/EBPα and C/EBPβ are required for sebocyte differentiation and stratified squamous differentiation in adult mouse skin. *PLoS One* **5**, e9837.

[49] Kariya Y, Kariya Y, and Gu J (2009). Roles of laminin-332 and $\alpha_6\beta_4$ integrin in tumor progression. *Mini Rev Med Chem* **9**, 1284–1291.

[50] Frijns E, Sachs N, Kreft M, Wilhelmsen K, and Sonnenberg A (2010). EGF-induced MAPK signaling inhibits hemidesmosome formation through phosphorylation of the integrin β_4. *J Biol Chem* **285**, 37650–37662.

[51] Lipscomb EA and Mercurio AM (2005). Mobilization and activation of a signaling competent $\alpha_6\beta_4$ integrin underlies its contribution to carcinoma progression. *Cancer Metastasis Rev* **24**, 413–423.

[52] Litjens SH, de Pereda JM, and Sonnenberg A (2006). Current insights into the formation and breakdown of hemidesmosomes. *Trends Cell Biol* **16**, 376–383.

[53] Soung YH, Gil HJ, Clifford JL, and Chung J (2011). Role of $\alpha_6\beta_4$ integrin in cell motility, invasion and metastasis of mammary tumors. *Curr Protein Pept Sci* **12**, 23–29.

[54] Streuli CH and Akhtar N (2009). Signal co-operation between integrins and other receptor systems. *Biochem J* **418**, 491–506.

[55] Merdek KD, Yang X, Taglienti CA, Shaw LM, and Mercurio AM (2007). Intrinsic signaling functions of the β_4 integrin intracellular domain. *J Biol Chem* **282**, 30322–30330.

[56] Yang X, Kovalenko OV, Tang W, Claas C, Stipp CS, and Hemler MH (2004). Palmitoylation supports assembly and function of integrin-tetraspanin complexes. *J Cell Biol* **167**, 1231–1240.

[57] Giancotti FG (2007). Targeting integrin β_4 for cancer and anti-angiogenic therapy. *Trends Pharmacol Sci* **28**, 506–511.

[58] LaFlamme SE, Homan SM, Bodeau AL, and Mastrangelo AM (1997). Integrin cytoplasmic domains as connectors to the cell's signal transduction apparatus. *Matrix Biol* **16**, 153–163.

[59] Yang X, Dutta U, and Shaw LM (2010). SHP2 mediates the localized activation of Fyn downstream of the $\alpha_6\beta_4$ integrin to promote carcinoma invasion. *Mol Cell Biol* **30**, 5306–5317.

[60] Gagnoux-Palacios L, Dans M, van't Hof W, Mariotti A, Pepe A, Meneguzzi G, Resh MD, and Giancotti FG (2003). Compartmentalization of integrin $\alpha_6\beta_4$ signaling in lipid rafts. *J Cell Biol* **162**, 1189–1196.

[61] Pankov R, Endo Y, Even-Ram S, Araki M, Clark K, Cukierman E, Matsumoto K, and Yamada KM (2005). A Rac switch regulates random *versus* directionally persistent cell migration. *J Cell Biol* **170**, 793–802.

[62] Pullar CE, Baier BS, Kariya Y, Russell AJ, Horst BA, Marinkovich MP, and Isseroff RR (2006). β_4 Integrin and epidermal growth factor coordinately regulate electric field–mediated directional migration via Rac1. *Mol Biol Cell* **17**, 4925–4935.

[63] Marinkovich MP, Lunstrum GP, and Burgeson RE (1992). The anchoring filament protein kalinin is synthesized and secreted as a high molecular weight precursor. *J Biol Chem* **267**, 17900–17906.

[64] Schenk S, Hintermann E, Bilban M, Koshikawa N, Hojilla C, Khokha R, and Quaranta V (2003). Binding to EGF receptor of a laminin-5 EGF-like fragment liberated during MMP-dependent mammary gland involution. *J Cell Biol* **161**, 197–209.

[65] Gagnoux-Palacios L, Allegra M, Spirito F, Pommeret O, Romero C, Ortonne JP, and Meneguzzi G (2001). The short arm of the laminin γ_2 chain plays a pivotal role in the incorporation of laminin 5 into the extracellular matrix and in cell adhesion. *J Cell Biol* **153**, 835–850.

[66] Sigle RO, Gil SG, Bhattacharya M, Ryan MC, Yang TM, Brown TA, Boutaud A, Miyashita Y, Olerud J, and Carter WG (2004). Globular domains 4/5 of the laminin α_3 chain mediate deposition of precursor laminin 5. *J Cell Sci* **117**, 4481–4494.

[67] Tripathi M, Nandana S, Yamashita H, Ganesan R, Kirchhofer D, and Quaranta V (2008). Laminin-332 is a substrate for hepsin, a protease associated with prostate cancer progression. *J Biol Chem* **283**, 30576–30584.

[68] Ogura Y, Matsunaga Y, Nishiyama T, and Amano S (2008). Plasmin induces degradation and dysfunction of laminin 332 (laminin 5) and impaired assembly of basement membrane at the dermal-epidermal junction. *Br J Dermatol* **159**, 49–60.

[69] Esselens CW, Malapeira J, Colomé N, Moss M, Canals F, and Arribas J (2008). Metastasis-associated C4.4A, a GPI-anchored protein cleaved by ADAM10 and ADAM17. *Biol Chem* **389**, 1075–1084.

[70] Simons M and Raposo G (2009). Exosomes—vesicular carriers for intercellular communication. *Curr Opin Cell Biol* **21**, 575–581.

[71] Staubach S, Razawi H, and Hanisch FG (2009). Proteomics of MUC1-containing lipid rafts from plasma membranes and exosomes of human breast carcinoma cells MCF-7. *Proteomics* **9**, 2820–2835.

[72] Jiang A, Lehti K, Wang X, Weiss SJ, Keski-Oja J, and Pei D (2001). Regulation of membrane-type matrix metalloproteinase 1 activity by dynamin-mediated endocytosis. *Proc Natl Acad Sci USA* **98**, 13693–13698.

[73] Escrevente C, Morais VA, Keller S, Soares CM, Altevogt P, and Costa J (2008). Functional role of *N*-glycosylation from ADAM10 in processing, localization and activity of the enzyme. *Biochim Biophys Acta* **1780**, 905–913.

[74] Hakulinen J, Sankkila L, Sugiyama N, Lehti K, and Keski-Oja J (2008). Secretion of active membrane type 1 matrix metalloproteinase (MMP-14) into extracellular space in microvesicular exosomes. *J Cell Biochem* **105**, 1211–1218.

Table W1. Antibodies, Matrix Proteins, and Inhibitors.

(A) Antibodies

C4.4 (anti-rC4.4A)	[1]
D5.7 (anti-rEpCAM)	[1]
B5.5 (anti-r$\alpha_6\beta_4$) (not WB)	[1]
Anti-hC4.4A	[2]
Anti-rpanCD44 (clone Ox50)	European Association of Animal Cell Cultures, Porton Down, United Kingdom
Anti-ruPAR	American Diagnostica, Pfungstadt, Germany
Anti-ruPA	American Diagnostica, Pfungstadt, Germany
Anti-rMMP2	Dianova, Hamburg, Germany
Anti-rMMP9	Dianova, Hamburg, Germany
Anti-rTACE	Stressgen, Ann Arbor, MI
Anti-rMMP14	Santa Cruz Biotech, Heidelberg, Germany
Anti-rHIF-1α	Santa Cruz Biotech, Heidelberg, Germany
Anti-rβ4	BD, Heidelberg, Germany
Anti-actin	BD, Heidelberg, Germany
Anti-FN	BD, Heidelberg, Germany
Anti-rLN111	BD, Heidelberg, Germany
Anti-hLNγ2 (crossr. rat)	BD, Heidelberg, Germany
LSα3 (anti-hLNα3 chain)	[3]
8A (anti-hLNβ3 chain)	[3]
D4B5 (anti-hLNγ2 chain)	[3]
Anti-mouse, anti-rabbit, anti-hamster IgG (HRP-, biotin-, fluorescent dye-labeled)	Dianova, Hamburg, Germany

(B) Matrix Proteins

Fibronectin (Sigma, Munich, Germany)	2 µg/ml
Rat LN111 (Sigma, Munich, Germany)	5 µg/ml
Rat LN332 (804G exosome-depleted culture supernatant w/o FCS)	50 µg/ml
Human LN332 (A431 exosome-depleted culture supernatant w/o FCS)	50 µg/ml

(C) Inhibitors

Aprotinin (serine protease inhibitor) (Sigma, Munich, Germany)	10 µM
MMP9/13-inhibitor-II (MMP-Inh.II) (Merck, Darmstadt, Germany)	3 µM
TAPI (TACE inhibitor) (Merck, Darmstadt, Germany)	40 µM

References

[1] Matzku S, Wenzel A, Liu S, and Zöller M (1989). Antigenic differences between metastatic and nonmetastatic BSp73 rat tumor variants characterized by monoclonal antibodies. *Cancer Res* **49**, 1294–1299.

[2] Paret C, Hildebrand D, Weitz J, Kopp-Schneider A, Kuhn A, Beer A, Hautmann R, and Zöller M (2007). C4.4A as a candidate marker in the diagnosis of colorectal cancer. *Br J Cancer* **97**, 1146–1156.

[3] Nakashima Y, Kariya Y, Yasuda C, and Miyazaki K (2005). Regulation of cell adhesion and type VII collagen binding by the β_3 chain short arm of laminin-5: effect of its proteolytic cleavage. *J Biochem* **138**, 539–552.

Table W2. Primers.

Hif for: CCACAGGACAGTACAGGATGC
Hif rev: GCAGCTCGTGTCCTCAGATT
C4.4A for: CTACAGCTG CGTGCAAAAGG
C4.4A rev: GTTGAGTTTGGCGTTGCAT
β-actin for: TCATGAAGTGTGACGTTGACATCCGT
β-actin rev: CCTAGAAGCATTTGCGGTGCACGATG.

Table W3. HRE in the C4.4A Promoter.

HRE in the C4.4A promoter

TTATTTTTTTCTTCAAGCTCTGGGGATAGGATCAGGGCTTCATCCACACCAGGCAAACCAT
CAAACTTCCCTTTTTCATTTGGAAGACTGCCCAGTGACCCCAGTCTTCCTGCGCCCTTTAT
CAAGCCTGGGGAGGAGTTTGAAATAGGGTCTCACTATGTAGCTCAGGCTGGCTTCAAACT
CAATACAATCCTGTCTGAGCTTCCTAAGTCTAGAATTTTAAGCAGGAGCCATTATACCCA
GCCCTCCCTTCCTCCCTCTCCCTCCCTGCCCTCCATTCTTGTTTTTATCACTCTTGATTTCTC
TGCAGGTTCATTGTCTAGGGTCTGTGATTCTGTCTCATTACATTTATTTATTTATTCATTAC
TTGGAGTTGTGGTACAGATATGTGGAAGGCAGAAGATACTTCTTAGGAATCAATTCTTGT
GTCTCTCTTTCTACCATGTGGGTTCCAGGGATCCAACTCGGGCCCTCAGGTTGGAGACAG
GCGTTTTTACATGCGAACCATGTCACACACACACACACACACACACACACACACACACAC
CCATATACAGTCTCTCTATGCAGCCCAGACTCCGGTCAAACTTAGGTTCTGTCTTGGCCTC
CTA**CGTG**CTGAACTACAGGGAAGCCCTGGCTCAGCTTCCCAATGTACAACCAGTGAAGA
TCTAAGTATGCGGCCGGCCGATGCTGTAGATTGTACATCACAGGCACACACACAAGGCCAC
CCTCCCTAGAAGGAAATGGAAGAGGCATCTTCCAGGACAAGACTCTCTGAGAGGGAACC
TCTATTCGTTTTCTAAACTGACCCATTTCTGTGGGTTAGATTGGACTGTTTCAGAACTCCA
CATAAAAGTCACACTGTGCGCTGCCTTGCTTCTGGTTTCATCGAGTCATTGTTTTAAAGAT
CCATCTATGTAGCTGTATACACCATCCACTGAAACCTTCCATTGCTAAGCGACAGTGCAT
GGGGTGGAGGGACCACT**CGTG**GTTTTATTACTCAATTAATTAATTATTTATTGAATCAGG
CGATGTTGGGGATGGACCCCAGGGCTTCGTTCATGCTGAGTGAGTGCTTTACCACTAAGC
CTTAAGTACTACCATCTCTCACTGAGGGAATCTAGGCAGGGGCTCTACCACTGAGCCACG
CCCCCAGCCCCTCACTGGGGGATTCTAGGCAGGGGCTCTACCACTGAGCCACGCCCCCAG
CCCCTCACTGGGGGATTCTAGGCAGGACTCCACTGCTGACCCCTAATGCACTATCCGAAC
TCTCCAACCACTATTTTTTTTTTTAATTTAAAGGACTTATTAGAGTGCCCAGCACACATGA
TAGTTGTGCAAGACTTGTTTTCATTTTTTATTCATTTTTTGAGACTTTCAGCCATGTTTGCA
ATGTATTTTGATCTATATACCTTTCTTATCACCTCTCGATAGATACCCGATATTATTTCCCA
GCTTAATCATATTGAAAAGTCTACTTCTCAATTTCAGCTCGA**CGTG**TAGCCCTTTATCCGT
ATTCCTCCACAGCCTTAATCTCTTGTAAGTCATAACCCACTTGTTTGTTTTGGCTTTTTGAG
ATAAGATCTCTTTCTGTAGTTCAGTGAGACCTGGAATCACCATGCCTCAAACTCATGGCA
ATCCTCCTGCCTCAGCTCCATGAGTGCTGTGATTACAGGCATGAGTCACCACGCCTGACTT
GTAAATAACAGTTTTCCCAATTATTTAATTAATATCTGTATCTGCCATCAGACTGGGAGCT
CTGCGAAGACAGACAGTAGTTCTGCCCCAGGGTCGCCAGTCCCCGAGCGAAGGCAGGCA
GGCGGGCACACCGCAAAAGCTCAGGCCCCTAGCAGACCCTGAATGTCCCTGTCTCTCTTT
GAACCCTGGTACTTCCTCTGCCTCTGAAACCCACACATACTTTTATCCAGGGGACTGGAG
GGAACCTCTACTCCCGCCCTTTCCCTTCTTGGCAAAGGCACAGGGCAGGGGCCGCTCTCC
CTGTGGGTGACGCACCTAGAGGCGGGCCCGCCCCACAGCGGACGCTGAGTTGGCCTGGTT
GGGCAAGGCCAGGGTTGCCCCGGGGTAGGTTACTCATCTAAGGCTCAGGTAAGAGGGCC
CGGGTTGGAAGGTGGCACACCCAGGGGGGACTCGGAGAGAGCAGGACACAGCT**ATG**

Boldface emphasis indicates the start codon; **bold blue**, HRE1 (–673 bp); **bold green**, HRE2 (–1183 bp); **bold red**, HRE3 (–1557 bp).